Macromolecular Materials and Engineering
www.mme-journal.de

Cross-Linkable Modified Nanocellulose/Polyester Resin-Based Composites: Effect of Unsaturated Fatty Acid Nanocellulose Modification on Material Performances

Jelena D. Rusmirović, Milica P. Rančić, Vladimir B. Pavlović, Vesna M. Rakić, Sanja Stevanović, Jasna Djonlagić, and Aleksandar D. Marinković*

Unsaturated fatty acid (FA)–modified nanocellulose (m-NC) shows potential application in improving mechanical properties of unsaturated polyester/m-NC nanocomposites (UPe/m-NC). A polyester matrix is obtained by polycondensation of maleic anhydride and products of poly(ethylene terephthalate) depolymerization with propylene glycol. Two methods of NC modification are performed: direct esterification with oleic acid, linseed, or sunflower oil FAs, and esterification/amidation with maleic acid/ethylene diamine (MA/EDA) bridging group followed by amidation with methyl ester of FAs. Increases of stress at break in the ranges from 148.8% to 181.4% and from 155.8% to193.0% for UPe/m-NC composites loaded with 1 wt% of NC modified directly or via MA/EDA cross-linker, respectively, are obtained. Results of the modeling of tensile modulus, by using the Cox–Krenchel model, show good agreement with experimentally obtained data. The effect of FAs' cross-linking capabilities on the dynamic-mechanical and thermal properties of the UPe/m-NC is studied. Cross-linking density, modulus, and T_g of the nanocomposite show appropriate relation with the unsaturation extent/structure of NC modification.

Dr. J. D. Rusmirović
Innovation Center
Faculty of Technology and Metallurgy
University of Belgrade
Karnegijeva 4, 11060 Belgrade, Serbia
E-mail: jrusmirovic@tmf.bg.ac.rs
Dr. M. P. Rančić
Faculty of Forestry
University of Belgrade
Kneza Višeslava 1, 11131 Belgrade, Serbia
Prof. V. B. Pavlović, Prof. V. M. Rakić
Faculty of Agriculture
University of Belgrade
Nemanjina 6, 11080 Belgrade, Zemun, Serbia
Prof. V. B. Pavlović
Institute of Technical Sciences of the SASA
Knez Mihailova 35/IV, 11000 Belgrade, Serbia
Dr. S. Stevanović
ICTM
Department of Electrochemistry
University of Belgrade
Karnegijeva 4, 11000 Belgrade, Serbia
Prof. J. Djonlagić, Dr. A. D. Marinković
Faculty of Technology and Metallurgy
University of Belgrade
Karnegijeva 4, 11060 Belgrade, Serbia

DOI: 10.1002/mame.201700648

1. Introduction

Polymer-based composites play an important role in the modern industry including automotive, aerospace, marine, sporting goods, and electronics. A large interest has grown in composites based on thermosetting polymer matrices reinforced with renewable natural fillers such as lignocellulosic materials, nanocrystalline cellulose (NC), and cellulosic fibers.[1–6] The unique high crystalline and well-defined NC structure with one dimension in nanometer range, as well as high aspect ratio, high mechanical properties, rigidity, tensile strength (0.3–22 GPa),[6] and modulus (138–150 GPa), makes NC a valuable filler in reinforcing polymer.[5,7] Unsaturated polyester (UPe) resins represent the most frequently used nonpolar thermosetting matrices for fiber-reinforced composites,[8,9] including NC-reinforced polymer composites, due to high strength and modulus, high resistance to water, room temperature cure capability, and transparency.[1] Moreover, UPe obtained from waste poly(ethylene terephthalate) (PET) can be mixed with the reactive vinyl monomer,[10] and further used for production of composites reinforced with NC. In addition, natural filler-reinforced composites based on recyclable polymer matrices have a positive economic and environmental outlook,[8] considering that the applying cycle of reusable and renewable materials for high-performance composites will be rounding out.[11]

Some of the major disadvantages of the NC-reinforcing filler include moisture absorption, and its polar and hydrophilic nature, which inhibit homogeneous dispersion in nonpolar polymer matrices.[12–14] Besides reducing NC's hydrophilic nature, the bonding strength between cellulose filler and UPe thermosetting resin is one of the most important factors for obtaining good reinforcement in the composite.[11,15] In recent years, many techniques for chemical surface modification of NC have been considered in order to improve dispersibility, compatibility, and bonding (interactions at the interface) with nonpolar polymer matrices.[16–19] The esterification of NC with fatty acids (FAs) and derivatives isolated from natural vegetable oils (VO) stands out as "green one-pot" methods of surface NC modification;[20–23] and one of the major benefits of the FAs' esterified

NC results in improved thermal stability, smaller agglomerate particle sizes, and significantly more hydrophobic surface than the unmodified one.[24] The widespread use of VO derivatives has gain increasing attention as the most promising renewable materials for the synthesis of polyols, especially polyurethanes and thermoplastic poly(ester urethanes) (TPEU),[25,26] linear/cross-linked polymers of different types, e.g., polyesters, as well as for composites' production based on thermosetting resins. The presence of vinyl double bonds in FAs provides wealth chemical transformation applicable for cationic, free radical, or olefin metathesis polymerization.[27] Isolated or conjugated double bonds can participate in free radicals' reaction with UPe/vinyl monomer systems in that way contributing to the significant improvement of mechanical properties of composites. NC modification with tall oil based on saturated, unsaturated, and branched FAs causes increase in thermal stability and retain maximum strain and elastic modulus comparable to the values of commercial products.[28] However, the incorporation of more reactive double bonds through chemical modification of VOs/FAs with maleic anhydride (MA) makes them more suitable for free radical polymerization[29] causing an improvement of elasticity and flexural modulus of the composites by nearly 50%.[15]

In this work, modified nanocellulose (m-NC) with unsaturated FAs was used as reactive reinforcement able to improve mechanical properties of produced UPe/m-NC nanocomposites. UPe polymer was synthesized from hydroxy functionalized product, obtained by catalytic PET glycolysis with propylene glycol (PG) without azeotropic removal of ethylene glycol and maleic anhydride. NC modification was performed by either direct esterification with oleic acid (OA), linseed acid (LO), or sunflower oil (SO) FAs, or by amidation of MA/ethylene diamine (MA/EDA) with FA methyl esters in order to obtained cross-linkable functionalities. The main aim of this study was related to investigate of the effect of vinyl cross-linkable groups at m-NC surface on the morphological, dynamic-mechanical analysis (DMA), and thermal properties of the UPe/m-NC nanocomposites.

2. Experimental Section

2.1. Materials

Cotton used for NC isolation was supplied from AD. Niva, Serbia (Turkish origin). The following chemicals were supplied from Sigma Aldrich: H_2SO_4, ethanol, methanol, glacial acetic acid (GAA), toluene, HCl, perchloric acid, MA, OA, tetrahydrofurane (THF), ethylenediamine (EDA), potassium hydroxide (KOH), diethyl ether, sodium sulfate, pyridine, *p*-toluenesulfonyl chloride, dicyclohexylcarbodiimide (DCC), dichloromethane (DCM), 4-dimethylaminopyridine (DMAP), styrene, 2-butanone peroxide (methyl ethyl ketone peroxide; MEKP), cobalt octoate (Co-oct), and potassium bromide (KBr). Commercial carbon dioxide (99.99% purity) and nitrogen (99.99% purity) were supplied by Messer-Tehnogas (Serbia). Propylene glycol (1,2-propanediol), xylene (mixture of 1,2-, 1,3-, and 1,4-dimethyl-benzene), and tetrabutyltitanate (TBT) were supplied by Fluka. All the chemicals used in this study were of analytical grade and used as received. Waste PET, used for unsaturated polyester resin production, was collected from soft beverage bottles. PET bottles were crushed into small pieces (≈0.5 × 0.5 cm), and then washed with ethanol and DCM to remove impurities and residual adhesives.

2.1.1. Cellulose Nanocrystals Isolation

Procedure for NC isolation[11] is presented in the Supporting Information.

2.2. Isolation of FAs and Preparation of Methyl Esters of FAs

Procedure for isolation of FAs from LO and SO, named FALO and FASO, respectively, as well as for preparation of methyl esters of LO, SO, and soybean oil (SOYA), named MELO, MESO, and MESY, was previously described in detail[11] and presented in the Supporting Information.

2.3. Chemical Modification of NC with FAs and Methyl Esters of FAs

Direct bonding of FAs, done according to the procedure described elsewhere,[11] was performed on NC isolated from water suspension (containing 2 g of dry residue) by washing/centrifuging three times with methanol and pyridine. The obtained residue was transferred into a three-necked round-bottomed flask of 250 mL equipped with nitrogen inlet and air drying tubes. Afterward, 100 mL of pyridine, 3.5 g of *p*-toluenesulfonyl chloride, and 5 mL of OA or isolated FAs were added to the flask. The reaction mixture was mixed by the magnetic stirrer and heated at 50 °C for 2 h, and after that 100 mL of absolute ethanol was added and the reaction was terminated. Removal of residual solvent and reactants was achieved by repeating of three cycles of centrifugation (5 min at 6000 rpm) and redispersion 15 min at ultrasound (Bandelin Electronic, Berlin, Germany, power 120 W, frequency 35 kHz) in absolute ethanol.

Modification of NC with methyl esters of FAs was done in a two-step process via MA/EDA cross-linker (amino-terminated moiety at NC surface obtained by amidation of MA residue with EDA). MA/EDA modification of NC (see the Supporting Information), performed according to the previously described procedure,[30] gave a product named NC-MA/EDA. Then, in the second step, NC-MA/EDA was modified with methyl esters of FAs by the following procedure.[11] About 2 g of NC-MA/EDA was placed in a 250 mL three-necked flask and dispersed in 50 mL of toluene in an ultrasonic bath (Bandelin electronic, Berlin, Germany, power 120 W, frequency 35 kHz); afterward, 5 g of methyl esters of FA solution in THF was added dropwise. The reaction mixture was stirred and heated for 2 h with the magnetic stirrer at 50 °C. The reaction product was washed with absolute ethanol using repeated centrifugation/sonication cycles, and dried under supercritical CO_2 (SCD drying) condition in a semibatch Autoclave Engineers Screening at 40 °C and at a pressure of 20 MPa. Two drying steps, 1 h without supercritical CO_2 ($scCO_2$) flow and 2 h with continuous $scCO_2$ flow (425 g h^{-1} flow rate),[11] were applied. The abbreviations of obtained m-NC samples were as follow: NC-bare NC, NC-OA,

NC-FALO, and NC-FASO-directly linked OA, FALO, and FASO onto NC, respectively; NC-MELO, NC-MESO, and NC-MESY–methyl esters of FALO, FASO, and FASY linked via MA/EDA cross-linker onto NC surface.

2.4. Synthesis of UPe Resin

UPe was synthesized from MA and products, obtained by PET depolymerization with PG in the presence of TBT catalyst, according to the procedure presented in the previous work.[31,32] Following the glycolysis procedure described earlier,[31,32] molar ratio of PET and PG used for glycolysis was 1:2.2 and the reaction was maintained at 210 °C. After the completion of the glycolysis reaction, keeping inert atmosphere, the mixture was cooled down to 90 °C and the Dean–Stark separator was assembled. MA (123 g, 1.25 mol) and 0.03 g of hydroquinone (HQ) dissolved in 2 mL of ethanol were charged, whereupon the mixture was heated to 115 °C at a constant temperature for 1 h. Afterward, continuous temperature increase was achieved at a heating rate of 15 °C h^{-1} until 150 °C, when the toluene azeotropic removal of water was started. The temperature increase was continued until 210 °C. The reaction was conducted until the acid number value decreased below 30 mg KOH g^{-1}, after which the resin obtained was cooled down to 120 °C and a solution of 0.03 g HQ in 2 mL of methanol was added. After purification product by vacuum distillation, the resin was dissolved in styrene (40 wt%). It was demonstrated in the previously work,[31] applying NMR analysis, that the dominant products of UPe synthesis were glycol esters of terephthalic acid: *bis*(2-hydroxylpropyl) terephthalate, (2-hydroxyethyl)(2-hydroxypropyl) terephthalate, and residual glycols (PG and ethylene glycol). The molar mass of the synthesized macromolecular UPe resin, determined from the hydroxyl and acid numbers values, was 2634 g mol^{-1}.[31] The obtained UPe resin was used as polymer matrix in m-NC composite preparation.

2.5. Preparation of Composites

SCD-dried unmodified and m-NC at different weight percentages were homogenized with 3 g of UPe resin for 20 min, followed by the addition of an accelerator/initiator system and continued with mechanical mixing and ultrasonic treatment (Bandelin electronic, Berlin, Germany, power 120 W, frequency 35 kHz) (10 min/2 min, respectively). The curing accelerator/initiator system consisted of 0.5 wt% cobalt octoate as the accelerator and 1 wt% of methyl ethyl ketone peroxide as the initiator. Afterward, the composite mixtures were molded into standard molds, cured at room temperature for 12 h, and then postcured at 80 °C for 6 h. Obtained composites were named as UPe/m-NC(*n*). Index (*n*) designates the weight percent of the m-NC addition: 0.5 wt%(a), 1.0 wt%(b), and 2.0 wt%(c).

2.6. Characterization Methods and Computational Details

The structural analysis of the UPe/m-NC nanocomposites (UPe/m-NC) was performed by Fourier transform infrared (FTIR) (Bomem MB-102) spectroscopy, within a range of 400–4000 cm^{-1}, at a resolution of 4 cm^{-1} and in ten scan mode. The prepared procedure was consisted of sample homogenization with KBr (1% of sample) and compression of homogenized mass into pill using laboratory hydraulic press.

Microstructural (morphological) characterization of nanocomposites was performed with a transmission electron microscope (TEM) JEM-1400.

Uniaxial tensile measurements of standard cured samples (standard dimension: 60 × 10 × 4 mm, with a narrow neck area: 15 × 4 × 4 mm) (ASTM D882)[33] were performed using an AG–X plus Universal testing machine, Shimadzu. All tests were performed at room temperature and were adjusted at a crosshead speed of 0.5 mm min^{-1}. Differential scanning calorimetry coupled with thermogravimetry (DSC-TG) was used to study thermal behavior of investigated samples. The experiments were performed using the TG/DSC 111 from Setaram, consisting of a quartz microreactor heated in a vertical furnace. Approximately 2 mg of each sample was heated from 25 up to 600 °C with a heating rate of 5 °C min^{-1}. The experiments were carried out in helium (flow rate = 30 cm^3 min^{-1}).

Raman spectra, recorded in the range 3400–100 cm^{-1}, were collected with aXploRA Raman spectrometer from Horiba JobinYvon. The system employed laser at 532 nm (maximum output power = 20–25 mW). All the measurements were realized using the spectrometer equipped with a 2400 g mm^{-1} grating. The Raman spectrometer was connected with an optical microscope equipped with a motorized stage.

A NanoScope III A (Veeco, USA) microscope was used to study the morphology of modified NC suspension on the mica surface by atomic force microscopy (AFM), which operated in contact mode under ambient conditions. Silicon nitride probes were used. Samples were prepared by applying a 10 μL of absolute ethanol suspension on freshly clean mica plate.

The mechanical properties and glass transition temperature (T_g) of UPe/m-NC composites were obtained by using dynamic-mechanical analysis, which was performed on a Discovery Hybrid Rheometer HR2 (TA Instruments). The DMA was conducted in a torsion rectangular mode (sample dimensions: 6/1/0.2 cm) from 25 to 220 °C at a fixed strain amplitude of 0.1% and an angular frequency of 1 Hz. The results were presented as mechanical spectra by monitoring the dependence of the storage shear modulus (G') and loss shear modulus (G'') and loss or damping factor tanδ (G''/G').

Segment of m-NC particles and UPe macromolecule was built in VegaZZ 3.0.5.[34] Structures of (*E*)-but-2-ene, dimethyl terephthalate, methyl (*E*)-4-((2-acetamidoethyl)amino)-4-oxobut-2-enoate, and (*Z*)-4-methoxy-4-oxobut-2-enoic acid were built separately in the Vega, and then manually connected to the modified NC and UPe macromolecule. Structures of adducts were minimized in NAMD 2.9, using a conjugate gradient algorithm, during 1000 steps. CHARMm22 force field was used. The semiempirical PM6 method[35] was used to ascribe atomic charges. Molecular electrostatic potential of the each adduct was visualized by VegaZZ.

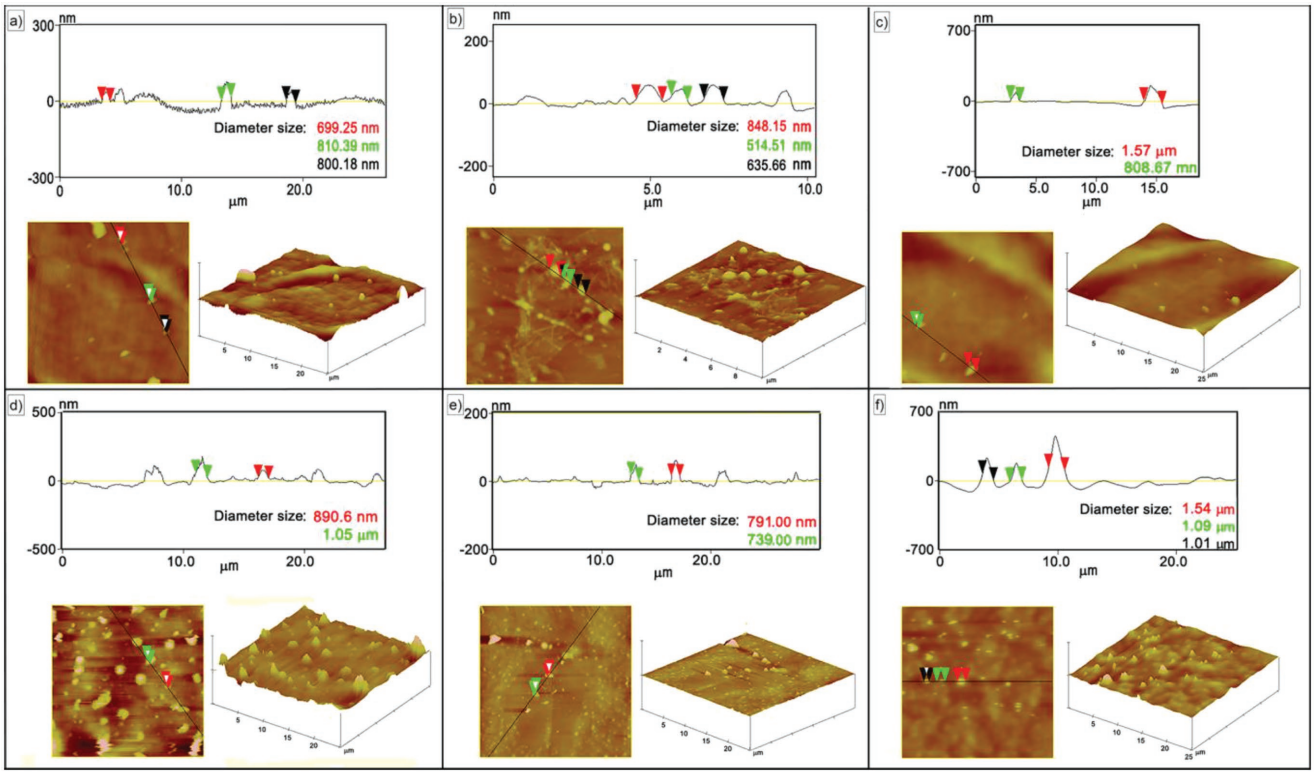

Figure 1. 2D, 3D AFM image and height profiles of a) NC-OA, b) NC-FASO, c) NC-FALO, d) NC-MELO, e) NC-MESO, and f) NC-MESY nanoparticles.

3. Results and Discussion

3.1. AFM of NC after Chemical Treatment

The AFM images of modified NC particles are presented on **Figure 1**. Comparing the obtained representative values of length and diameter size of NC directly modified by FAs and NC modified by FAs via MA/EDA cross-linker with the length and diameter of the bare NC,[11] it can be concluded that both modification procedures cause formation of spherical agglomerates. Average representative values of length and diameter, determined for NC-OA, NC-FASO, and NC-FALO, were 781.2, 1603.0, and 1189.3 nm; and 769.9, 666.1, and 1152.1 nm, respectively. For NC-MELO, NC-MESO, and NC-MESY, similar values of lengths (765.0, 970.0, and 1213.3 nm), and diameters (756.8, 927.7, and 1111.1 nm), respectively, were determined. The evaluated representative length and diameter of m-NC were used as input parameters in modeling of tensile modulus of the nanocomposites using the Cox–Krenchel model (Section 3.5).

3.2. FTIR Analysis of Cured Nanocomposites

FTIR spectra of cured nanocomposites were presented in **Figure 2**a,b. The broad peak at about 3479 cm^{-1} and the low-intensity peak at 700 cm^{-1} originate from hydroxyl (OH) groups' stretching vibrations. An increase in intensity and width of the OH groups' stretching vibrations peak in the FTIR spectra of cured UPe/m-NC(b) nanocomposites is observed due to hydrogen bonding (**Figure 3**) between the UPe macromolecular chains and m-NC.[36] The highest extent of hydrogen bonding interaction appears at 1.0 wt% of NC modified with methyl esters of FAs via MA/EDA cross-linker due to its better dispersibility and larger contact area between filler surface and UPe chains. The bands in the region 3084–3028 cm^{-1} correspond to the valence aromatic C—H stretching vibrations. Overlapped symmetric and asymmetric stretching, and bending vibrations of methyl and methylene groups are observed at 2982, 2937, and 1454 cm^{-1}, respectively. The band at 1728 cm^{-1} originates from carbonyl (C=O) groups present in terephthalic acid ester. Skeletal C=C double bond vibrations observed at 1645–1602 cm^{-1} correspond to phenyl core. Two narrow adsorption peaks identified at about 731 and 700 cm^{-1} are assigned to the skeletal γ(CH) phenyl core vibrations. Ester C—O stretching vibrations, asymmetric and symmetric, are observed at about 1383 and 1117 cm^{-1}, respectively.

3.3. Curing Kinetics Analysis Using Raman Spectroscopy

Intensities of Raman bands in the region 1900–1300 cm^{-1} of the reacting system, UPe, styrene, and m-NC at the initial point, after 30, 60, and 90 min of cross-linking and postcuring for 6 h at 80 °C are presented in Figure 2c–f. Raman spectra were normalized in relation to 1725 cm^{-1} band, and characteristic Raman bands are listed in Table S1 (Supporting Information). The intensity of the styrenic C=C band at 1625 cm^{-1} decreases during the polymerization. This band disappears almost completely from the spectra of all postcured samples, while vinyl C—H band at 1409 cm^{-1} originated from styrene also decreases.[37] Moreover, the intensity of the saturated

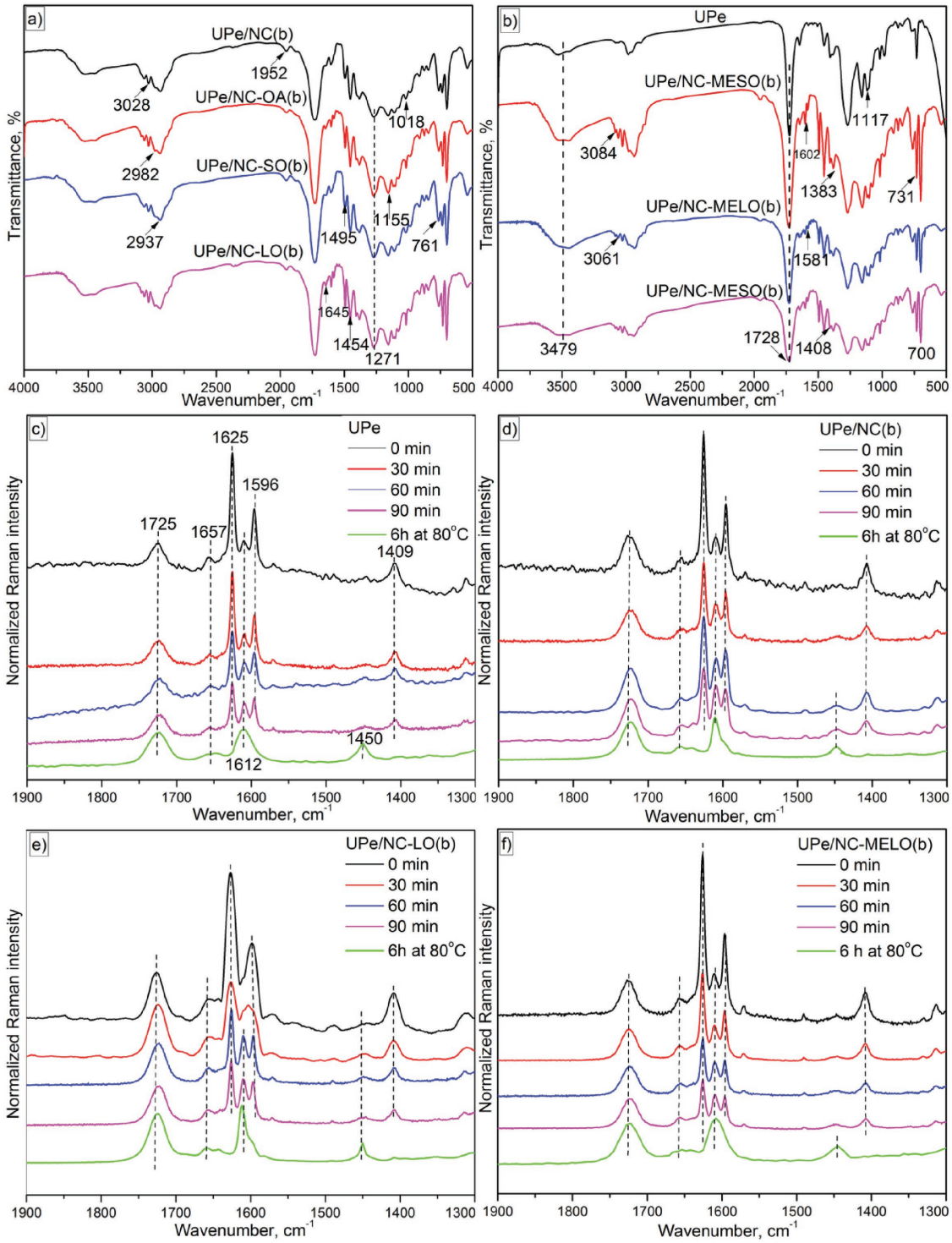

Figure 2. a,b) FTIR and c–f) Raman spectra of cured UPe and UPe/m-NC(b) nanocomposites.

C—H band at 1450 cm^{-1} increases slightly as a result of participation of vinyl groups in the cross-linking reaction with concomitant transformation to saturated C—H groups. The conversion rate, $\alpha(t)$, of neat UPe and selected UPe/m-NC(b) was calculated according to Equation (1), and obtained results are given in **Table 1**.

$$\alpha(t) = \frac{(I_0 - I_t)}{I_0} \quad (1)$$

where I_t presents peak height of vinyl C=C band after the period t and I_0 presents peak height of vinyl C=C band at the moment of addition of curing catalyst system.

Macromolecular Materials and Engineering
www.mme-journal.de

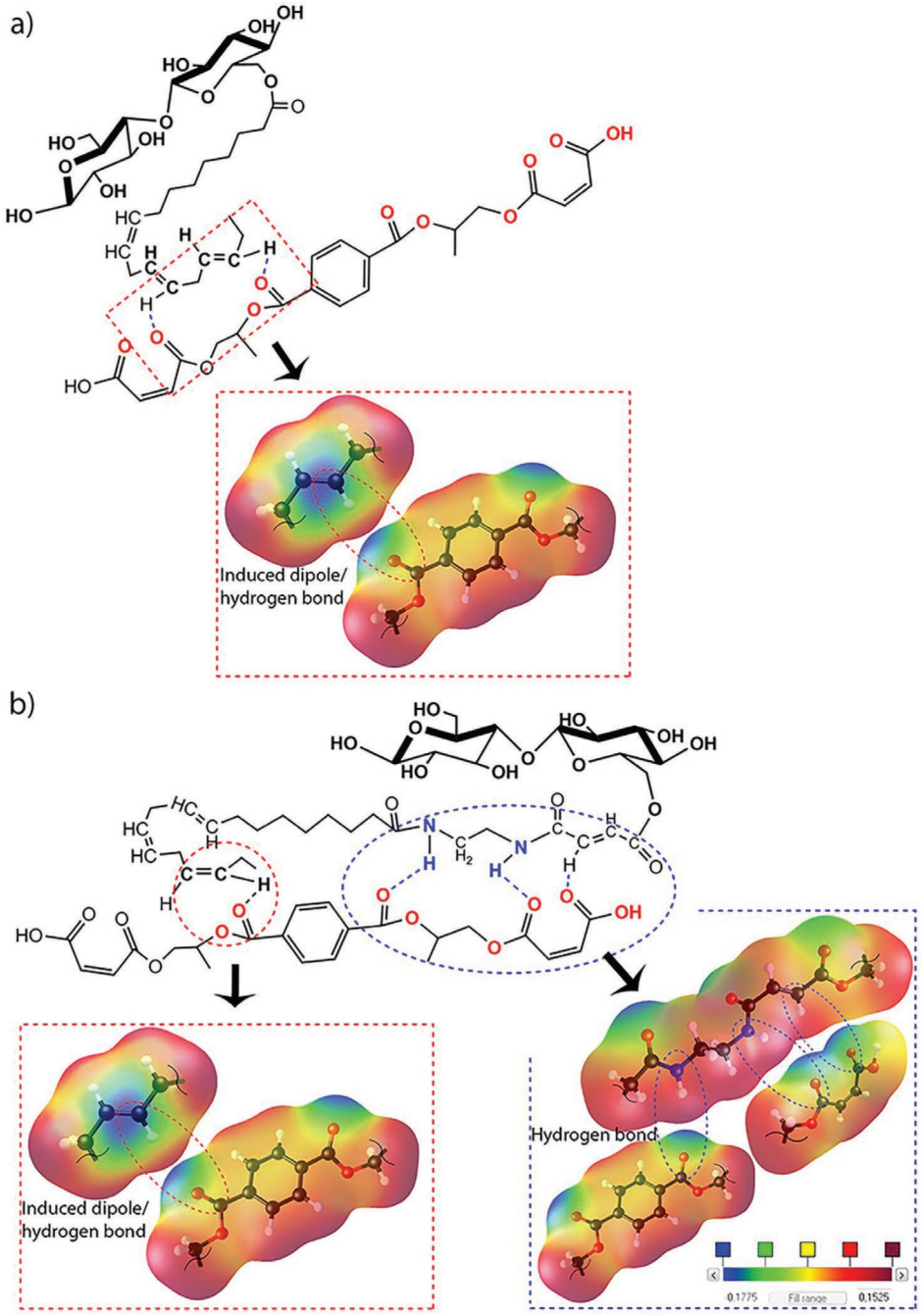

Figure 3. a,b) Schematic illustration of possible intermolecular interaction between UPe and m-NC particles.

Table 1. The conversion rate values ($\alpha(t)$) of neat UPe and UPe/m-NC nanocomposites.

$\alpha(t)$	UPe	UPe/NC(b)	UPe/NC-LO(b)	UPe/NC-MELO(b)
$\alpha(0)$	0.0	0.0	0.0	0.0
α(30 min)	0.33	0.22	0.48	0.47
α(60 min)	0.44	0.48	0.58	0.66
α(90 min)	0.52	0.57	0.59	0.71
α(6 h at 80 °C)	0.99	0.99	0.99	0.99

Generally, m-NC loading causes an increase of the cross-linking rate in the first 90 min. Exception is UPe/NC(b) for 30 min of curing, while postcuring at 80 °C for 6 h additionally contributes to achievement of the high extent of cross-linking processes ($\alpha(t) \approx 0.99$). However, a small peak at 1409 cm^{-1}, observed even after postcuring, indicates the presence of low amount of unreacted styrene/double bonds in UPe.[38]

Faster reaction rate of styrene homopolymerization, with respect to complex copolymerization processes of UPe/styrene/m-NC,[39] causes nonuniform reactivity of the system,

and due to concomitant shrinkage, the process result in residual styrene monomer/oligomer captured in final product. The highest conversion rate in first 90 min was found for UPe/NC-MELO(b).

3.4. TEM Analysis of Nanocomposite Materials

TEM images of cured nanocomposites, shown in **Figure 4** and Figure S1 (Supporting Information), indicate that m-NCs form interlaced densely packed laminar agglomerated structures as a consequence of strong H-bonding among cellulose nanocrystals.[40] TEM images of the UPe/NC-OA(b), UPe/NC-LO(b), and UPe/NC-SO(b) (Figure 4a–c) show the presence of the NC agglomerates of higher dimensions (≈1.174 µm), compared to the composites loaded with m-NC modified via MA/EDA cross-linker (≈0.967 µm, Figure 4d–f). Formation of larger agglomerates is a consequence of lower extent of intermolecular interactions with UPe macromolecular chains (Figure 3). Cross-linkable functionalities in MA/EDA bridging group and FA residues contribute to higher extent of reactivity and intermolecular interactions influencing more homogeneous m-NC distribution in latter nanocomposites. The highest level of homogeneity was observed in UPe/NC-MELO(b) and UPe/NC-MESY(b).

3.5. Mechanical Testing of UPe/m-NC Nanocomposite Materials

The mechanical testing results and stress–strain curves of the examined cured nanocomposites are shown in **Table 2** and Figure S2 (Supporting Information), respectively. The results were evaluated using the Cox–Krenchel mechanical model, and

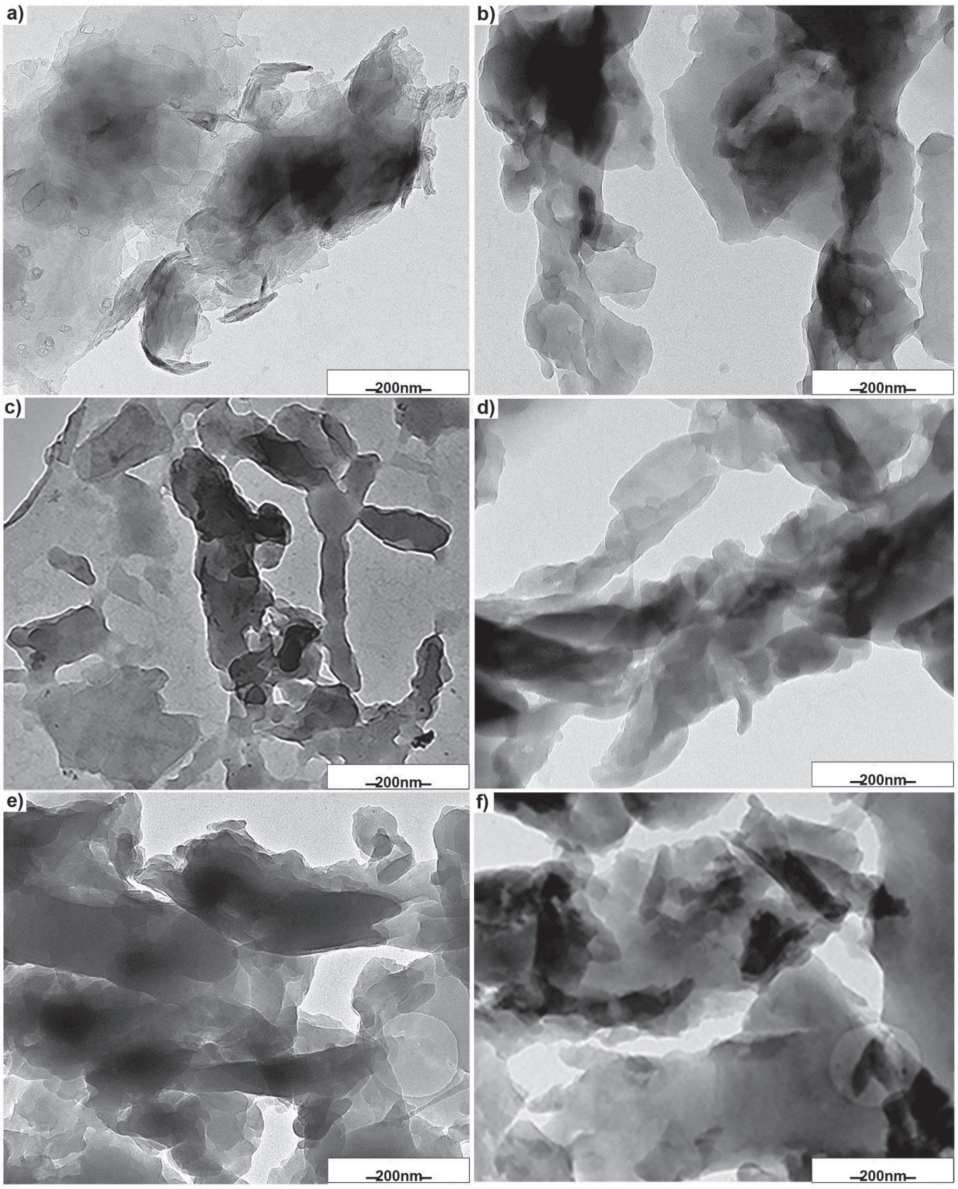

Figure 4. TEM image of a) UPe/NC-OA(b), b) UPe/NC-LO(b), c) UPe/NC-SO(b), d) UPe/NC-MELO(b), e) UPe/NC-MESO(b), and f) UPe/NC-MESY(b).

Table 2. Stress at break (σ_b), elongation at break (ε), experimental values of tensile modulus (E_{exp}), tensile modulus determined using the Cox–Krenchel model (E_{cox}), and energy adsorption values (EA) of cured UPe/m-NC nanocomposites.

Sample	σ_b [MPa]	ε [%]	E_{exp} [GPa]	E_{cox} [GPa]	EA [J cm^{-3}]	Sample	σ_b [MPa]	ε [%]	E_{exp} [GPa]	E_{cox} [GPa]	EA [J cm^{-3}]
UPe	43 ± 1.4	2.8	1.8	–	63.8	UPe	43 ± 1.4	2.8	1.8	–	63.8
UPe/NC-OA(a)	64 ± 1.9	3.5	1.9	1.6 (–19%[a])	121.0	UPe/NC-MELO(a)	78 ± 1.8	3.9	2.1	1.6 (–31%[a])	160.9
UPe/NC-OA(b)	76 ± 1.9	3.9	2.0	1.8 (–11%[a])	154.9	UPe/NC-MELO(b)	81 ± 1.6	4.5	1.9	1.7 (–12%[a])	195.0
UPe/NC-OA(c)	71 ± 1.8	4.1	1.8	2.1 (+14%[a])	146.8	UPe/NC-MELO(c)	79 ± 1.8	4.1	2.0	2.1(+4.8%[a])	174.0
UPe/NC-LO(a)	66 ± 1.6	2.8	2.3	1.6 (–44%[a])	100.7	UPe/NC-MESO(a)	67 ± 1.5	3.4	2.0	1.6 (–25%[a])	123.5
UPe/NC-LO (b)	81 ± 1.6	5.4	1.6	1.8 (+11%[a])	172.5	UPe/NC-MESO(b)	82 ± 1.7	4.5	1.8	1.8 (/[a])	196.6
UPe/NC-LO (c)	75 ± 1.6	3.9	1.9	2.2 (+14%[a])	166.4	UPe/NC-MESO(c)	75 ± 1.4	3.4	2.2	2.2 (/[a])	130.6
UPe/NC-SO(a)	64 ± 1.3	2.9	2.2	1.7 (–29%[a])	96.7	UPe/NC-MESY(a)	72 ± 1.3	3.3	2.2	1.7 (–29%[a])	94.5
UPe/NC-SO(b)	79 ± 1.7	4.5	1.8	2.0 (+10%[a])	192.6	UPe/NC-MESY(b)	83 ± 1.8	5.5	1.5	1.9(+21%[a])	261.8
UPe/NC-SO(c)	69 ± 1.7	3.4	2.0	2.5 (+20%[a])	127.6	UPe/NC-MESY(c)	74 ± 1.8	3.9	1.9	2.2(+14%[a])	150.5

[a]Deviation from experimental determinate E_{exp} values.

values of tensile modulus (E_{cox}) are given in Table 2. Numerical computation using MATLAB7.11.0 program was done according to the algorithm and input data shown in Figure S3 and Equation (S1) in the Supporting Information.

Similar values of stress at break (σ_b), elongation at break (ε), and tensile modulus (E_{exp}) of nanocomposites with nanofiller are obtained via esterification with OA and SO fatty acids. Tensile properties are sensitive probe to various types of intermolecular/interfacial interactions, e.g., N—H/O—H and O—H/O—H hydrogen bond, between UPe macromolecular chains and m-NC,[13] as depicted in Figure 3. As an example, residues of OA contain one unsaturated double bond on C9 atom suitable for copolymerization with UPe matrix, and participate in a formation of weak induced dipole/hydrogen bond (Figure 3).

Moreover, higher ε values, in comparison to pure UPe, are a consequence of introduction of soft-flexible segments of OA and SO fatty acids in UPe/m-NC composites. FA residues at m-NC surface exert appropriate level of plasticizing effect in obtained product. Somewhat higher values of tensile properties obtained for UPe/NC–LO could be attributed to the highest content of linolenic acid.[27] Possible participation of a number vinyl bonds (three per linolenic unit) in a copolymerization contributes to higher cross-linking density and with contribution of higher extent of dipole/induced dipole interaction (Figure 3) causes an appropriate increase of σ_b. Incorporation of MA/EDA cross-linker causes an increase of σ_b values in composite with 1 wt% loading of NC particles (UPe/m-NC(b)). This behavior can be explained by additional contribution of N—H/O hydrogen bonding (Figure 3). The influence of the content of m-NC nanofiller on the σ_b of UPe/m-NC change is shown in **Figure 5**a,b. The highest value was found for UPe/NC-MESY(b). Energy absorption (EA) results (Table 2, Figure 5c,d)) show the influence of the type and addition level of m-NC on the change of the EA of the nanocomposites. EA values increase with higher addition of m-NC up to 1 wt%, and then slightly decrease.

Results of tensile modulus, from Cox–Krenchel modeling (E_{cox}; Table 2), showed good agreement with experimentally obtained ones. The used modeling method with appropriate selection of input parameters provided good description of the tensile properties of analyzed/similar materials.

Literature data on mechanical properties of UPe-based nanocomposites, reinforced with NC filler (Table S2, Supporting Information), showed significant improvement in relation to unmodified NC/UPe composites (example: 55 MPa with 0.5 wt% of NC filler; Table S2, Supporting Information). However, the results obtained in this work showed even more pronounced improvement of σ_b due to higher reactivity, influenced by increased content of vinyl groups at NC surface/styrene/UPe reacting system, in the course of nanocomposites curing, and thus higher cross-linking density is a consequence. Appropriate relation of σ_b change, comparing UPe reinforced with NC modified with FAs either directly or via MA/EDA cross-linker, with respect to the content of C=C bonds introduced by MA moiety in MA/EDA linker, was noticed (example: UPe/NC-SO(b)-79 MPa versus UPe/NC-MESO(b)-82 MPa).

3.6. Dynamic-Mechanical Analysis of UPe/m-NC Nanocomposite Materials

The temperature dependences of storage modulus (G'), which reflects elastic behavior, and loss modulus (G''), which reflects viscous behavior of cured nanocomposites, are given in **Figure 6** and Figure S4 (Supporting Information), respectively. **Table 3** shows a summary of the G' in the glassy (G'_{GS}) and in the rubbery (G'_{RP}) regions at 50 and 180 °C, as well as peak height (tanδ), glass transition temperature determined from tanδ peak position ($T_{g(\tan\delta)}$) and cross-linking density (ν) determined according to Equation (2)

$$\nu = \left(G'_{RP}\right)/RT \tag{2}$$

where R is the universal gas constant and T is T_g + 30 °C.

The storage modulus in glassy regions shows no significant change for pure UPe resin and all studied nanocomposites. The G'_{GS} changes provide information on the thermomechanical properties as results of overall intermolecular/interfacial interactions in UPe/m-NC systems. Low variation of the G'_{GS} values

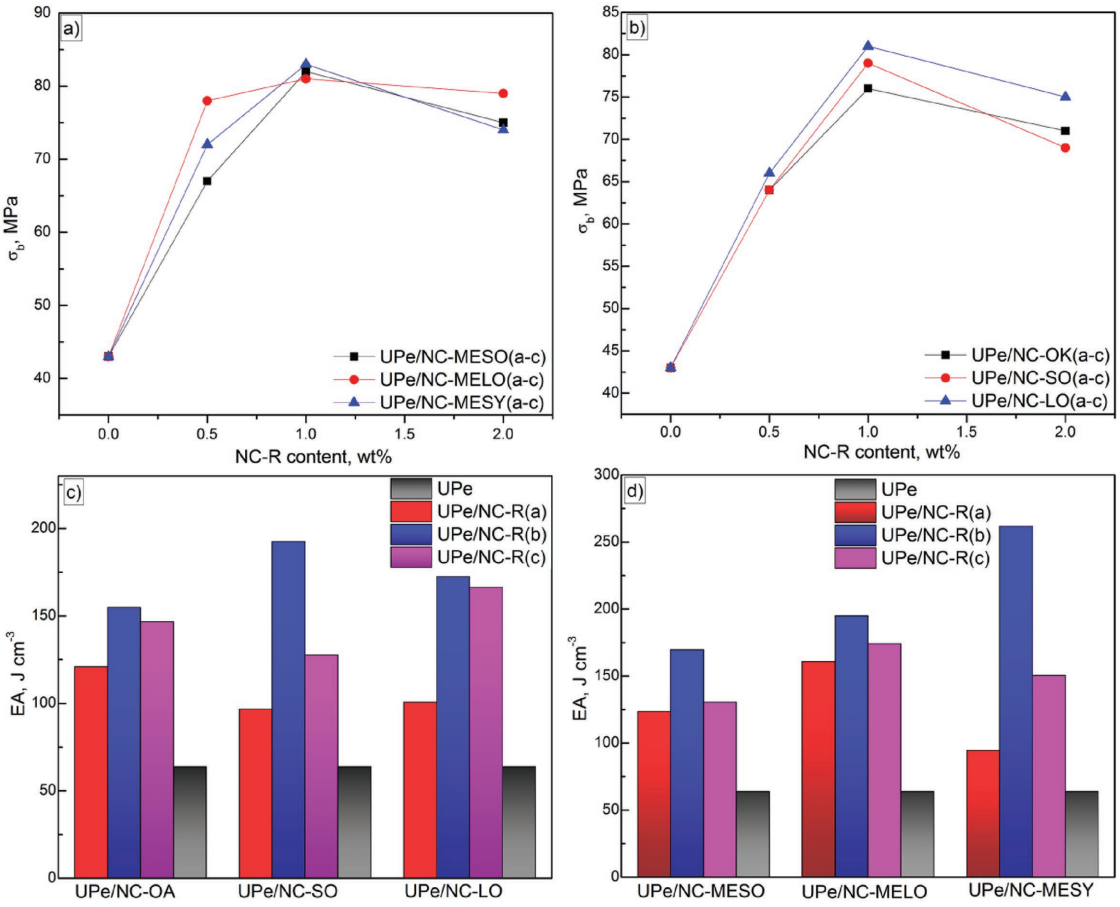

Figure 5. Influence of m-NC content on the stress at break of a,b) UPe/NC-R and c,d) energy absorption as a function of m-NC structure for tensile tests.

with NCs loadings up to 2.0% (Figure S4, Supporting Information) is a result of low capability of the NCs filler to prevent free movement of polymeric chains/molecular fragments to a greater extent at low temperature. It could be the result of low fraction of the m-NC reinforcing filler added. Furthermore, in the rubbery plateau, considering the region that appears at higher temperatures (T > 180 °C) (Figure 6; Figure S4, Supporting Information), the lower values of G'_{RP} are observed in all nanocomopsites with 1.0% loading of both unmodified and m-NCs. Only for the UPe/NC-MESY(b) sample, the higher G'_{RP} value is observed probably due to the formation of stiff cellulose networks governed by percolation threshold associated with tangling effects within the material.[41] From the temperature dependences of G'', two peaks can be observed (Figure 6b; Figure S4b, Supporting Information). The peaks at lower temperature, in the range of 55–95 °C, induce the presence of microphases as a result of heterogeneous composition of UPe matrix that relaxes in the subglassy state. Peaks observed in the range of 107–150 °C originate from polymer transition from glassy to rubber state. $T_{g(\tan\delta)}$ and tanδ values, determined for pure UPe resin and UPe/m-NC nanocomposites, are presented in Table 3. All cured UPe/m-NC nanocomposites have lower $T_{g(\tan\delta)}$ and tanδ values. Decrease in tanδ values with incorporation of a filler is usually promoted by the restriction of the free movement of the polymer chain segments.[42] Generally, increased level of unsaturation on m-NC surface contributes to higher cross-linking density in the corresponding composite. The lowest cross-linking density is found for the UPe/NC-SO(b) sample, while the highest for UPe/NC-MESY(b).

3.7. Thermal Analysis of UPe/m-NC Nanocomposite Materials

Thermal decomposition profiles of nanocomposites showed mass losses in different steps (Figure 6d). In the first step, at temperatures ≤ 200 °C, mass loss is a result of the removal of low amount of residual styrene and the low-boiling reactants. The mass loss, observed between 200 and 450 °C, corresponds to the decomposition of the polymer network and high-temperature thermal reactions/degradation processes which produce condensed/degraded carbonaceous materials.[32] Intermolecular interactions between UPe/m-NC, m-NC, and volatile decomposition products[41] have appropriate influence on thermal properties. The temperature corresponding to initial 5% mass loss ($T_{5\%}$) is an indicator of the removal processes of loosely bound low-boiling fraction of residual reactants and moisture. Degree of unsaturation, determined from detailed structural characterization of modified NC particles,[11] has also appropriate influence on $T_{5\%}$. The mass loss at $T_{5\%}$ of UPe/NC(b) samples is related to the ability of OH groups of

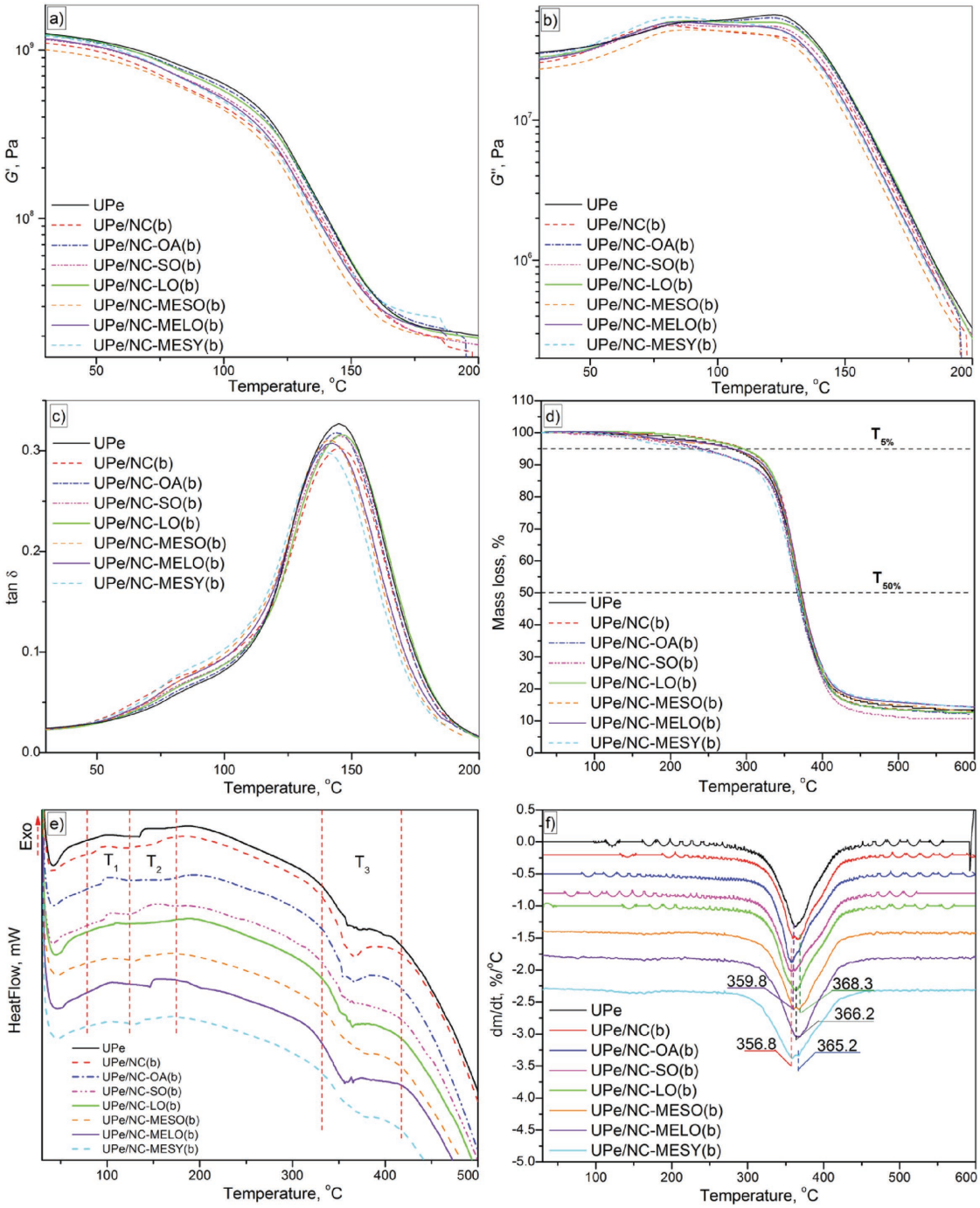

Figure 6. Temperature dependence of a–c) storage modulus (G'), loss modulus (G''), and tanδ. d–f) TGA/DTG curves and DSC thermograms of UPe and UPe/m-NC(b) nanocomposites.

unmodified NC to create hydrogen bond with OH groups of the glycol esters of terephthalic acid and residual glycols (Section 2.4). The low influence of NC functionalization on decomposition temperature at 50% mass loss ($T_{50\%}$) indicated similar thermal stability/degradation processes of the nanocomposites studied. Final mass loss (m loss) of 87.02% for cured unreinforced UPe was obtained at 600 °C. Higher values were obtained for UPe/NC(b), UPe/NC-OA(b), UPe/NC-SO(b), and UPe/NC-LO(b), while lower were obtained for other nanocomposites. The DSC results of cured UPe/m-NC nanocomposites are shown in **Table 4** and in Figure 6e).

DSC thermograms of cured nanocomposites display two low-intensity peaks at temperature <200 °C, i.e., overlapped exothermic and endothermic peaks, and one higher intensity endothermic peak between 350 and 375 °C. Overlapped DSC peaks at lower temperatures could be ascribed to removal of

Table 3. Values of G'_{GS}, G'_{RP}, $T_{g(tan\delta)}$, tanδ, and ν of UPe and UPe/m-NC nanocomposites.

Sample	G'_{GS} [MPa]	G'_{RP} [MPa]	$T_{g(tan\delta)}$ [°C]	tanδ height	$\nu \times 10^3$ [mol cm^{-3}]
UPe	1100	23.6	151.3	0.32	5.4
UPe/NC(a)	1050	23.5	145.0	0.33	6.3
UPe/NC(b)	989	19.6	145.0	0.30	5.3
UPe/NC(c)	1150	21.2	146.0	0.30	5.7
UPe/NC-OA(b)	1112	22.4	145.0	0.32	6.0
UPe/NC-SO(b)	1043	19.4	145.0	0.31	5.2
UPe/NC-LO(b)	1121	20.9	146.0	0.31	5.6
UPe/NC-MESO(b)	905	19.6	140.0	0.31	5.3
UPe/NC-MELO(b)	1053	21.6	142.0	0.30	5.8
UPe/NC-MESY(b)	1087	25.5	140.0	0.30	6.9

low-boiling reactants, rearrangement/relaxation of composite network, and absorption of energy due to intermolecular interactions between volatile products, m-NC and UPe. Moreover, small exothermic peaks indicate additional curing of residual polymer matrix monomers or residual matrix polymer/NC-FA chains.

Endothermic peak, observed at higher temperature, is a result of thermally induced degradation and transformation processes which depend on thermal stability of the bonds/structure.

4. Conclusion

The main goal of this work was related to syntheses of vinyl cross-likable NC containing unsaturated FA residues used as reinforcement in green UPe/m-NC composites. The effect of vinyl reactive FA or MA/EDA/FA residues at NC surface on the morphological, DMA, and thermal properties of the UPe/m-NC nanocomposites was studied. AFM experiments of FA-modified NC particles showed that modification types do not have significant influence on diameter of agglomerate. The rate of conversion, determined from Raman analysis, showed that vinyl modified NC increases the cross-linking speed in the first 90 min after addition of an accelerator/initiator system.

Table 4. $T_{5\%}$ and $T_{50\%}$ data, DSC endothermic and exothermic heat of the composites.

Sample	$T_{5\%}$[a)] [°C]	$T_{50\%}$[a)] [°C]	m loss[b)] [%]	T_1 [°C]	ΔH [J g^{-1}]	T_2 [°C]	ΔH [J g^{-1}]	T_3 [°C]	ΔH [J g^{-1}]
UPe	281.3	369.7	87.02	96.6	−12.3	134.8	24.0	359.5	131.0
UPe/NC(b)	294.3	371.6	87.74	94.1	−10.9	147.3	12	365.1	139.4
UPe/NC-OA(b)	244.3	367.1	87.91	100.6	−12.3	167.0	7.4	354.0	131.1
UPe/NC-SO(b)	239.4	367.7	87.37	102.2	−11.3	125.2	13.1	361.0	121.0
UPe/NC-LO(b)	294.3	370.4	89.26	109.4	−3.2	151.0	4.17	365.0	117.5
UPe/NC-MELO(b)	281.3	372.9	85.87	100.8	−5.5	134.0	10.3	375.0	84.0
UPe/NC-MESO(b)	281.3	372.9	85.65	112.5	−1.3	165.0	5.3	368.2	128.7
UPe/NC-MESY(b)	224.7	367.7	85.90	103.8	−6.9	146.2	10.6	362.0	100.3

[a)] $T_{5\%}$ and $T_{50\%}$ are the temperatures at 5% and 50% mass losses; [b)] m loss at 600 °C.

Cross-linkable double bonds introduced through direct or via MA/EDA esterification with FAs make m-NC more reactive in copolymerization with UPe matrix causing the increase of mechanical properties to percolation threshold at 1 wt% of m-NC addition. The increased compatibility of UPe/m-NC brought about increased tensile strength, similar thermal stability, and lower values of G'_{RP} as a result of cross-linking ability and properties of FAs at m-NC surface.

Supporting Information

Supporting Information is available from the Wiley Online Library or from the author.

Acknowledgements

The authors acknowledge financial support from Ministry of Education, Science and Technological development of Serbia, Project No. OI 172057.

Conflict of Interest

The authors declare no conflict of interest.

Keywords

hybrid polyester nanocomposites, mechanical properties, nanocellulose modification, waste PET recycling

Received: December 18, 2017
Revised: March 22, 2018
Published online: May 28, 2018

[1] H. Kargarzadeh, R. Sheltami, I. Ahmad, I. Abdullah, A. Dufresne, *Polymer* **2015**, *56*, 346.
[2] V. K. Thakur, M. K. Thakur, *Carbohydr. Polym.* **2014**, *109*, 102.
[3] T. Lu, S. Liu, M. Jiang, X. Xu, Y. Wang, Z. Wang, J. Gou, D. Hui, Z. Zhou, *Composites, Part B* **2014**, *62*, 191.
[4] T. Lu, M. Jiang, Z. Jiang, D. Hui, Z. Wang, Z. Zhou, *Composites, Part B.* **2013**, *51*, 28.
[5] H. M. Ng, L. T. Sin, T. T. Tee, S. T. Bee, D. Hui, C. Y. Low, A. R. Rahmat, *Composites, Part B.* **2015**, *75*, 176.
[6] K.-Y. Lee, Y. Aitomäki, L. A. Berglund, K. Oksman, A. Bismarck, *Compos. Sci. Technol.* **2014**, *105*, 15.
[7] H. Kargarzadeh, N. Johar, I. Ahmad, *Compos. Sci. Technol.* **2017**, *151*, 147.
[8] D. E. Nikles, M. S. Farahat, *Macromol. Mater. Eng.* **2005**, *290*, 13.
[9] S. Fakirov, *Macromol. Mater. Eng.* **2013**, *298*, 9.
[10] T. Kovačević, J. Rusmirović, N. Tomić, G. Mladenović, M. Milošević, N. Mitrović, A. Marinković, *Polym. Compos.* **2018**, https://doi.org/10.1002/pc.24827.
[11] J. D. Rusmirović, J. Z. Ivanović, V. B. Pavlović, V. M. Rakić, M. P. Rančić, V. Djokić, A. D. Marinković, *Carbohydr. Polym.* **2017**, *164*, 64.
[12] J. Lu, P. Askeland, L. T. Drzal, *Polymer* **2008**, *49*, 1285.
[13] S. Qian, K. Sheng, *Compos. Sci. Technol.* **2017**, *148*, 59.
[14] J. Sapkota, J. C. Natterodt, A. Shirole, E. J. Foster, C. Weder, *Macromol. Mater. Eng.* **2017**, *302*, 1600300.

[15] P. Kushwaha, R. Kumar, *J. Reinf. Plast. Compos.* **2010**, *30*, 73.
[16] H. Y. Yu, R. Chen, G. Y. Chen, L. Liu, X. G. Yang, J. M. Yao, *J. Nanopart. Res.* **2015**, *17*, 1.
[17] Z. L. Cheng, Q. H. Xu, Y. Gao, *Adv. Mater. Res.* **2012**, *627*, 859.
[18] M. de Oliveira Taipina, M. M. F. Ferrarezi, I. V. P. Yoshida, M. d. C. Gonçalves, *Cellulose* **2013**, *20*, 217.
[19] F. Ansari, M. Skrifvars, L. Berglund, *Compos. Sci. Technol.* **2015**, *117*, 298.
[20] Y. Yoo, J. P. Youngblood, *ACS Sustainable Chem. Eng.* **2016**, *4*, 3927.
[21] P. Uschanov, L. S. Johansson, S. L. Maunu, J. Laine, *Cellulose* **2011**, *18*, 393.
[22] E. V. Bryuzgin, V. V. Klimov, O. V. Dvoretskaya, L. D. Man', A. V. Navrotskiy, I. A. Novakov, *Russ. J. Appl. Chem.* **2014**, *87*, 1119.
[23] C. S. R. Freire, A. J. D. Silvestre, C. P. Neto, M. N. Belgacem, A. Gandini, *J. Appl. Polym. Sci.* **2006**, *100*, 1093.
[24] L. Wei, U. P. Agarwal, K. C. Hirth, L. M. Matuana, R. C. Sabo, N. M. Stark, *Carbohydr. Polym.* **2017**, *169*, 108.
[25] S. Li, L. Bouzidi, S. S. Narine, *Eur. Polym. J.* **2017**, *93*, 232.
[26] S. Shetranjiwalla, S. Li, L. Bouzidi, S. S. Narine, *J. Renewable Mater.* **2017**, *5*, 333.
[27] Y. Lu, R. C. Larock, *ChemSusChem* **2009**, *2*, 136.
[28] T. Kulomaa, J. Matikainen, P. Karhunen, M. Heikkilä, J. Fiskari, I. Kilpeläinen, *RSC Adv.* **2015**, *5*, 80702.
[29] E. Can, S. Küsefoglu, R. P. Wool, *J. Appl. Polym. Sci.* **2001**, *81*, 69.
[30] K. Taleb, J. Markovski, Z. Veličković, J. Rusmirović, M. Rančić, V. Pavlović, A. Marinković, *Arab. J. Chem.* **2016**.
[31] J. Rusmirović, K. Trifković, B. Bugarski, V. Pavlović, J. Džunuzović, M. Tomić, A. Marinković, *eXPRESS Polym. Lett.* **2016**, *10*, 139.
[32] J. Rusmirović, T. Radoman, E. Džunuzović, J. Džunuzović, J. Markovski, P. Spasojević, A. Marinković, *Polym. Compos.* **2017**, *38*, 538.
[33] ASTM D882–12, *Standard Test Method for Tensile Properties of Thin Plastic Sheeting*, ASTM International, West Conshohocken, PA **2012**.
[34] A. Pedretti, L. Villa, G. Vistoli, *J. Comput. Aided. Mol. Des.* **2004**, *18*, 167.
[35] J. J. P. Stewart, *J. Mol. Model.* **2007**, *13*, 1173.
[36] C. J. Chirayil, J. Joy, L. Mathew, J. Koetz, S. Thomas, *Ind. Crops Prod.* **2014**, *56*, 246.
[37] M. Skrifvars, P. Niemelä, R. Koskinen, O. Hormi, *J. Appl. Polym. Sci.* **2004**, *93*, 1285.
[38] D. S. Lee, S. H. Lee, J. H. Kim, *Polym. Int.* **1997**, *44*, 143.
[39] J. Grenet, S. Marais, M. T. Legras, P. Chevalier, M. J. Saiter, *J. Therm. Anal. Calorim.* **2000**, *61*, 719.
[40] P. Krishnamachari, R. Hashaikeh, M. Tiner, *Micron* **2011**, *42*, 751.
[41] H.-M. Ng, L. T. Sin, S.-T. Bee, T.-T. Tee, A. R. Rahmat, *Polym. Plast. Technol. Eng.* **2017**, *56*, 687.
[42] A. Lavoratti, L. C. Scienza, A. J. Zattera, *Carbohydr. Polym.* **2016**, *136*, 955.